Available online at www.sciencedirect.com

SCIENCE DIRECT®

Spectrochimica Acta Part A 60 (2004) 2601–2610

SPECTROCHIMICA ACTA PART A

www.elsevier.com/locate/saa

Spectrochemical, ab initio and density functional studies on the conversion of 2-hydroxybenzonitrile (*o*-cyanophenol) into the oxyanion

Yuri I. Binev*, Miglena K. Georgieva, Lalka I. Daskalova

Institute of Organic Chemistry, Bulgarian Academy of Sciences, 1113 Sofia, Bulgaria

Received 7 August 2003; accepted 18 December 2003

Abstract

The spectral and structural changes caused by the conversion of 2-hydroxybenzonitrile (*o*-cyanophenol) into the corresponding oxyanion have been followed by IR spectra, ab initio and density functional force field calculations. In agreement between theory and experiment, the conversion is accompanied by a 29 cm^{-1} frequency decrease of the cyano stretching band, 2.7-fold increase in its integrated intensity, 5.8-fold (total value) intensification of the aromatic skeletal bands of Wilson's *8* and *19* types, and other essential spectral changes. According to the calculations, the strongest structural changes are the shortening of the Ph–O bond with 0.10 Å, lengthenings of the adjacent CC bonds in the phenylene ring with 0.06 Å and bond angle variations *near* the oxyanionic center. All these changes are connected with the formation of a quasi-*ortho*-quinonoidal structure of the *o*-phenylene ring in the oxyanion. According to the electronic density analysis, 0.41 e^- (Mulliken) or 0.56 e^- (natural bond orbital, NBO) of the anionic charge remain localized at the oxyanionic center. Conformations and hydrogen bonds have also been discussed on the basis of experimental and theoretical data.

Keywords: IR; Ab initio; DFT; 2-Hydroxybenzonitrile (*o*-cyanophenol); Anion; Conformations; Hydrogen bonds

---

1. Introduction

Finkelstein and Willems reported as early as 1929 that 2-hydroxybenzonitrile, alone or with appropriate additives, can be used as a disinfectant, preservative, fungicide, parasiticide, etc. [1]. The general toxic action of 2-hydroxybenzonitrile has been repeatedly studied, e.g. [2–4], and herbicidal and insecticidal activities of its derivatives have also been proven [5,6]. There is over a hundred of patents describing 2-hydroxybenzonitrile as a precursor in the synthesis of medicines, e.g. for the treatment of thromboembolic disorders [7–9] and to enhance the anti-tumor activity of other cytotoxic agents [10], as drug delivery systems [11], modulators of neuropatic pains [12], etc.

Starting by Puttnam's work of 1960 [13], the IR studies of 2-hydroxybenzonitrile dealt mainly with its intra- and intermolecular hydrogen bondings in connection with the *s-cis*/*s-trans* preference of the molecule under various conditions [13–16]. Gebicki and Krantz found that the formation of $CO\cdots H–O–C_6H_4CN$ hydrogen bonds in solid argon matrices resulted in a 63 cm^{-1} decrease in $\nu_{O–H}$ and a 15 cm^{-1} increase in $\nu_{C=O}$ [17]. Complexes of 2-hydroxybenzonitrile with water and methanol have recently been studied using IR/UV double resonance and other techniques [18]. Detailed vibrational assignments of the three isomeric hydroxybenzonitriles were reported by Ram et al., quite a long time ago [19].

Vibrational spectra of the 2-hydroxybenzonitrile oxyanion have not been studied, so we believe the IR data for this anion will be of a special interest. We did not find in the literature any ab initio or DFT force field studies on the title species.

2. Experimental

We prepared 2-hydroxybenzonitrile **1** from salicylaldehyde **2**, according to the classical Meyer's procedure [20] (Scheme 1). The reaction of salicylaldoxime **3** with acetan-

---

* Corresponding author. Tel.: +359-2-739998; fax: +359-2-8700225.
E-mail address: yb@orgchm.bas.bg (Y.I. Binev).

1386-1425/$ – see front matter © 2004 Elsevier B.V. All rights reserved.
doi:10.1016/j.saa.2003.12.040

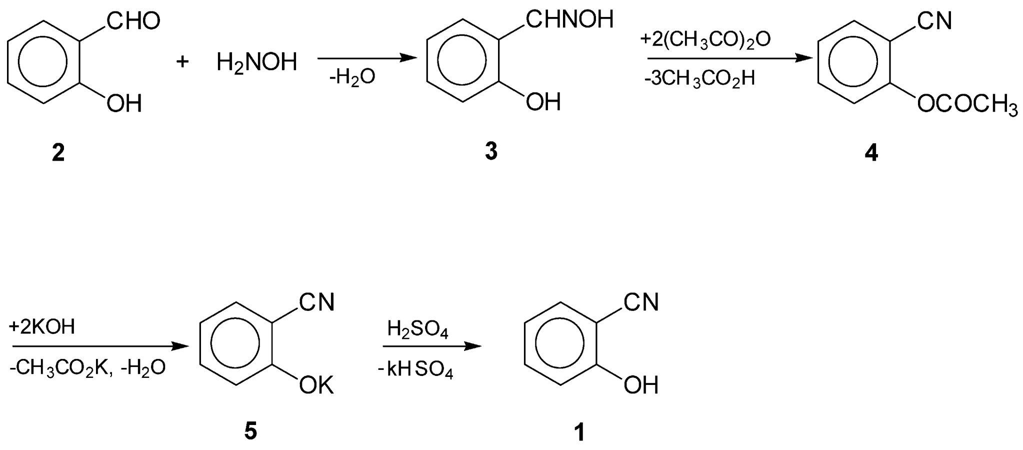

Scheme 1. Preparation of 2-hydroxybenzonitrile **1** from salicylaldehyde **2**.

hydride resulted in simultaneous conversion of the aldoxime group into cyano and the phenolic hydroxy one into acetoxy. Hydrolysis of the ester **4** by 10 wt.% KOH/aq. gave the potassium salt **5**, which reacted with 10 wt.% H_2SO_4/aq. to release the end product **1**. The reaction mixture was extracted by ether, the ethereal layer was washed, dried and the solvent evaporated. The residue was crystallized (m.p. 65 °C) after an overnight stay at 4 °C. Recrystallization from ethanol gave white crystals with m.p. 91 °C; their m.p. increased to 96 °C after a 2-day storage at −18 °C. The 2-hydroxybenzonitrile oxyanion **6** (counter ion Na^+) was prepared by adding 0.15 and 0.30 mol l^{-1} DMSO/DMSO-d_6 solutions of **1** to an excess of dry sodium methoxide-d_0 and -d_3 respectively, under argon. The conversion was practically complete: no bands of **1** were seen in the spectra after metalation. The dry sodium salt (**6**, counter ion Na^+) was prepared by reacting equivalent amounts of **1** and NaOH in water under argon, followed by evaporation of the solvent in vacuum. The IR spectra were measured on a Bruker IFS 113v FTIR spectrophotometer in a CaF_2 cell of 0.13 mm path length (for 0.15 and 0.30 mol l^{-1} DMSO/DMSO-d_6 solutions), a KBr cell of 0.18 mm path length (for 0.09 mol l^{-1} $CHCl_3$/$CDCl_3$ solutions), and KBr and CsI discs, at a resolution of 1 cm^{-1} and 50 scans.

3. Computations

The ab initio force field computations were performed by using the GAMESS software [21] (AIX version, 2000) at the HF [22] and MP2 [23] 6-31G(d) levels. The GAUSSIAN 98 program package [24] was used for the density functional BLYP [25], B3LYP [26] 6-31G(d) and B3LYP 6-31 + G(d,p) force field computations. All the computations were performed on a Pentium 2 PC, at a full geometry optimization. No scaling in the ab initio or density functional force fields was done. A standard least-square program was used for calculating the single-parameter linear regression indices; the theoretical spectra were simulated by means of the SimOpus [27] program.

4. Results and discussion

4.1. Energy analysis

The 2-cyanobenzonitrile molecule can exist as two conformers, *s-cis* **1a** and *s-trans* **1b** (Scheme 2). Their total energies and that of their oxyanion **6**, calculated by the five methods used, are compared in Table 1. Here are some comments on the data in Table 1:

1. According to all the calculations performed, **1a** is more stable than **1b** by 9.31–11.18 kJ mol^{-1}. This result is due to the formation of weak intra-molecular hydrogen bonds, known from experimental IR and NMR data [13–16], CNDO/2 [14], MNDO [28] and DFT [29] calculations. However, the two conformers coexist in solutions ([13–16] and the next sections). Having in mind the dipole moment value of 3.2 Debye [30], the *s-cis* conformer **1a** should be prevalent in carbon tetrachloride solutions (sections 4.2 and 4.3.1), and in the solid state, the conformation is firmly *s-trans* [31].
2. The deprotonation energy E^D of 2-hydroxybenzonitrile can be calculated as a difference between the ZPVE-corrected total energies of the anion **6** and that of the more stable conformer **1a** of the molecule, $E^D = E_{anion} - E_{molecule}$. The four methods used gave within the 6-31G(d) basis E^D values in the interval of 1410.24–1430.44 kJ mol^{-1}. The E^D values are related to the gas-phase acidities of Broensted acids and could be used as an approximate measure of their pK_a values in polar aprotic solvents, which solvate cations mainly, e.g. DMSO: higher E^D's → lower acidities → higher pK_a's, e.g. [32–39]. For example, there is a fair linear correlation between gas-phase ΔG_{acid} and DMSO pK_a values for 97 C–H acids of various structures [40].

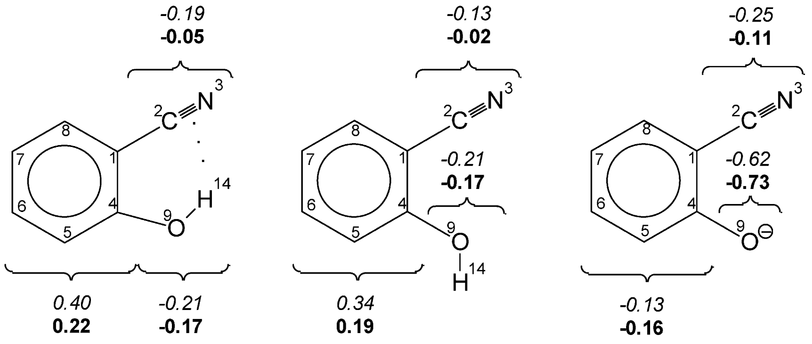

1a **1b** **6**

Scheme 2. Mulliken MP2 6-31G(d) (in italics) and natural bond orbital (NBO) B3LYP 6-31G(d) (in bold) total net electric charges over fragments of the *s-cis* **1a**, *s-trans* **1b** 2-hydroxybenzonitrile molecules of their oxyanion **6**.

Protic solvents, e.g. water, solvate both cations and anions, and modify strongly the Broensted acidity [41,42]. The pK_a value of 4-hydroxybenzonitrile in DMSO is 13.01–13.18 [38–40,43–45], however, we did not find in the literature of any pK_a data for DMSO solvent of the studied 2-hydroxybenzonitrile. So, we can compare the E^D values for the three hydroxybenzonitriles only with the corresponding pK_a's, measured in water, viz.: the pK_a value of 7.86 [41] for the studied *o*-isomer (see its E^D above) is close to that of 7.97 [41], for the *p*-isomer ($E^D =$ 1394.47–1419.37 kJ mol^{-1}, by the same methods [46]), quite lower than pK_a of 8.61 [47] and for the *m*-isomer ($E^D =$ 1414.99–1445.09 kJ mol^{-1}, using the same methods [46]).

Fortunately, however, the experimental E^D's of the isomeric hydroxybenzonitriles were known for a long time. They were determined by gas-phase proton-transfer equilibria, using a pulsed electron beam high-pressure mass spectrometer [48]. The following values were obtained in this manner (*isomer*, E^D in kJ mol^{-1}): *ortho*, 1384.3; *meta*, 1392.3; and *para*, 1378.0 [48]. These values could directly be compared (they should coincide) with the theoretical E^D's. In fact, however, the ab initio and DFT methods, applied within the 6-31G(d) basis set (this work and [46]), overestimated the deprotonation energies of hydroxybenzonitriles (cf. the above given E^D intervals) by the following mean deviations for the three isomers (method, mean deviation in kJ mol^{-1}): HF, 46.8; MP2, 28.5; BLYP, 21.7; and B3LYP, 28.7. The corresponding results, obtained on the basis of semi-empirical calculations were not very different from these just cited: MINDO/3, 96.4; MNDO, 29.0; and AM1, 17.3 [49]. It should be emphasized here that the E^D values of 1382.4 kJ mol^{-1} obtained for the title 2-hydroxybenzonitrile by means of the B3LYP 6-31 + G(d,p) method (cf. Table 1, last column), practically coincided with the experimental one (deviation of −1.9 kJ mol^{-1} only, cf. above).

4.2. Correlation analysis

In order to check which one among the methods used gave better description of the vibrational frequencies of the species studied, we compared their frequency predictions with our experimental data (sections 4.3.1 and 4.3.2). On the other hand, the correlation obtained could give some information about the prevalent conformer (**1a** or **1b**) of 2-hydroxybenzonitrile, like in the case of 3-amino-2-propenenitrile [38]. The results are summarised in Table 2 and we can see there, that:

1. As it can be expected [34–39,50,51], the DFT correlations are much better than the ab initio ones: they show largest *R* (correlation coefficient) smallest standard deviation (S.D.) and ρ (slope) parameters closed to 1, i.e.

Table 1
Native and ZPVE-corrected (values in italics) total energies (in hartree), calculated for the *s-cis* **1a** and *s-trans* **1b** 2-hydroxybenzonitrile conformers, and for their oxyanion **6**

No.	Structure	HF 6-31G(d)	MP2 6-31G(d)	BLYP 6-31G(d)	B3LYP 6-31G(d)	B3LYP 6-31 + G(d,p)
1	**1a**	−397.295980	−398.507809	−399.579164	−399.711788	−399.741249
2		*−397.184515*	*−398.405105*	*−399.478825*	*−399.608025*	*−399.637834*
3	**1b**	−397.292272	−398.504005	−399.574697	−399.707406	−399.737270
4		*−397.180968*	*−398.401535*	*−399.474565*	*−399.603866*	*−399.634037*
5	**6**	−396.736625	−397.955184	−399.028426	−399.158462	−399.200739
6		*−396.639545*	*−397.865900*	*−398.941554*	*−399.068427*	*−399.111074*

Table 2
Correlations between theoretical and experimental IR frequencies of *s-cis* **1a** and *s-trans* **1b** 2-hydroxybenzonitrile conformers, and of their oxyanion **6**, according to the equation $\nu_{\mathrm{exp.}} = \rho\nu_{\mathrm{theor.}} + b$ (cm^{-1})

No.	Species	Method	ρ[a]	b[b]	R[c]	S.D.[d]	n[e]
1	**1a**	HF 6-31G(d)	0.8786	26.9	0.9992	35.6	34
2		MP2 6-31G(d)	0.9203	70.1	0.9986	48.3	34
3		BLYP 6-31G(d)	0.9725	31.6	0.9992	35.9	34
4		B3LYP 6-31G(d)	0.9409	31.2	0.9995	27.9	34
5		B3LYP6-31 + G(d,p)	0.9353	42.5	0.9996	25.7	34
6	**1b**	HF 6-31G(d)	0.8723	37.8	0.9990	40.4	34
7		MP2 6-31G(d)	0.9140	81.0	0.9990	41.0	34
8		BLYP 6-31G(d)	0.9662	42.2	0.9996	25.9	34
9		B3LYP 6-31G(d)	0.9344	42.2	0.9997	22.0	34
10		B3LYP6-31 + G(d,p)	0.9291	52.8	0.9997	23.9	34
11	**6**	HF 6-31G(d)	0.9106	−13.7	0.9989	41.8	26
12		MP2 6-31G(d)	0.9356	50.8	0.9989	40.6	26
13		BLYP 6-31G(d)	0.9922	15.5	0.9997	21.9	26
14		B3LYP 6-31G(d)	0.9622	10.8	0.9996	24.1	26
15		B3LYP6-31 + G(d,p)	0.9609	18.0	0.9997	22.0	26

[a] Slope.
[b] Intercept.
[c] Correlation coefficient.
[d] Standard deviation.
[e] Number of data points.

the native (unscaled) DFT frequencies are closer to the experimental values.

2. The frequencies, calculated for the *s-trans* conformer **1b,** correlate better with the experimental ones (exception: HF), than those for **1a**. The sum of the S.D. values for the five methods used $\sum \mathrm{S.D.}\,(\mathbf{1b}) = 147.9\,\mathrm{cm}^{-1}$ is essentially smaller than $\sum \mathrm{S.D.}\,(\mathbf{1a}) = 162.3\,\mathrm{cm}^{-1}$ (cf. Table 2). The separate correlations for solvent DMSO/DMSO-d_6 (10 data points) and $\mathrm{CHCl_3/CDCl_3}$ (28 data points) (not included in Table 2) are also informative, as follows:

$$\text{solvent DMSO/DMSO-d}_6: \sum \mathrm{S.D.}\,(\mathbf{1b}) = 89.1\,\mathrm{cm}^{-1};$$

$$\sum \mathrm{S.D.}\,(\mathbf{1a}) = 109.0\,\mathrm{cm}^{-1}$$

$$\text{solvent CHCl}_3/\text{CDCl}_3: \sum \mathrm{S.D.}\,(\mathbf{1b}) = 159.3\,\mathrm{cm}^{-1};$$

$$\sum \mathrm{S.D.}\,(\mathbf{1a}) = 176.1\,\mathrm{cm}^{-1}$$

All these results can be explained in the following way: like in both cyclohexane and carbon tetrachloride solutions [13–16], **1a** and **1b** *coexist* also in the chloroform solutions studied (see also Section 4.3.1). In DMSO/DMSO-d_6 solutions **1b** should be strongly prevalent, due to the formation of strong intermolecular hydrogen bonds with the solvent mainly.

3. We shall use the ρ and b indices of correlations 6-15 (Table 2) for correlational scaling of the corresponding theoretical frequencies. As it was stated in Alcolea's review article [52], the use of scaling equations instead of scale factors gave better results, especially in the low-frequency region. Again according to Alcolea [52], the first scaling correlation equations appeared within 1992–1996 for AM1 [53] and ab initio [54–56] frequencies [53–56] and intensities [55,56]. This type of scaling is nowadays used frequently, e.g. [36–38,57,58].

The correlations between calculated and measured integrated intensities are poor, with R of 0.31–0.51 for **1a** and **1b**, and 0.32–0.45 for **6**. The S.D.'s of ca. 12.0 (**1a**), 11.6 (**1b)** and 51.3 (**6**) $\mathrm{km\,mol}^{-1}$ are larger than the intensities of many bands in the corresponding spectra, so these "correlations" could be used for some orientation only.

4.3. *Spectral analysis*

The IR spectra (1100–2300 cm^{-1}) of the molecule and anion studied are compared on Fig. 1. Let us first consider separately the spectra of the species studied, which will make it possible to follow the spectral changes, caused by the conversion of the 2-hydroxybenzonitrile molecule **1b** (see above) into the corresponding oxyanion **6**.

4.3.1. *The 2-hydroxybenzonitrile molecule* **1*b***

We compare the theoretical and experimental IR data for this molecule in Table 3. A good agreement can be seen there between experimental and theoretical frequencies. The mean absolute deviation (m.d.) between them for the ab initio calculations is ca. 27 cm^{-1}, which value is not away from the 15–25 cm^{-1} interval of deviations, typical for nitrile molecules [37] (and references therein). For the DFT calculations this deviation is ca. 18 cm^{-1}. This value is essentially smaller than the ab initio one and lies within the deviation interval of 9–20 cm^{-1}, found in cases of DFT calculations for five nitrile molecules [36–38,46].

Table 3
Theoretical (HF 6-31G(d), MP2 6-31G(d), BLYP 6-31G(d) and B3LYP 6-31G(d), 6-31 + G(d,p) force field) and experimental (solvent DMSO/DMSO-d_6) IR data for the *s-trans*-2-hydroxybenzonitrile molecule **1b**

No.	HF	MP2	BLYP	B3LYP	B3LYP[a]	B3LYP[a]	Approximate description[d]	Experimental[b]	
	ν (cm^{-1})[c]	ν (cm^{-1})[c]	ν (cm^{-1})[c]	ν (cm^{-1})[c]	ν (cm^{-1})[c]	A ($km\,mol^{-1}$)		ν (cm^{-1})	A ($km\,mol^{-1}$)
1	3650	3540	3525	3550	3609	80.5	$\nu_{O–H}$	3586[e,f]	13.6
								3559[e,g]	36.6
								3311[e,h]	189.7
2	3012	3075	3088	3058	3046	6.4	$\nu_{Ph–H}$	3076[e]	9.6
3	2995	3057	3075	3045	3034	5.8	$\nu_{Ph–H}$	3040[e]	1.5
4	2983	3045	3063	3034	3025	4.6	$\nu_{Ph–H}$	3021[e]	5.0
5	2979	3038	3039	3012	3005	9.2	$\nu_{Ph–H}$	2960[i]	w
6	2313	2102	2213	2238	2223	40.4	$\nu_{C\equiv N}$, $\nu_{C–CN}$	2223	24.6
7	1617	1622	1586	1596	1588	46.0	ν_{CC}, δ_{PhH}, δ_{CCC}	1603	20.0
8	1599	1610	1569	1579	1569	25.4	ν_{CC}, δ_{PhH}, δ_{PhoH}	1590	25.7
9	1501	1514	1492	1493	1481	36.2	δ_{PhH}, ν_{CC}, δ_{CCC}	1506	6.6
10	1451	1464	1443	1444	1433	62.9	δ_{PhH}, δ_{CCC}, ν_{CC}	1457	47.4
11	1313	1421	1344	1329	1321	30.1	δ_{PhH}, δ_{PhH}	1368	19.9
12	1274	1319	1298	1297	1289	89.4	$\nu_{Ph–O}$, δ_{PhH}, ν_{CC}	1275	13.0
13	1211	1294	1264	1264	1255	27.0	δ_{PhH}, δ_{PhOH}, ν_{CC}	1246	16.2
14	1181	1224	1202	1201	1194	27.9	δ_{PhH}, $\nu_{C–CN}$, δ_{CCC}	1215	48.4
15	1159	1192	1171	1165	1157	20.4	δ_{PhH}, ν_{CC}, δ_{PhOH}	1182	0.2
16	1107	1188	1168	1160	1155	25.1	ν_{CC}, δ_{PhH}, δ_{PhOH}	1160	5.7
17	1069	1112	1091	1091	1087	57.5	ν_{CC}, δ_{PhH}, δ_{PhOH}	1104	3.8
18	1030	1068	1042	1042	1040	2.8	ν, δ_{PhH}	1034[c]	4.5
19	1010	886	945	959	973	0.0	ν_{CC}, δ_{PhOH}, δ_{PhH}	945[c]	0.7
20	982	875	914	929	943	1.7	δ_{PhH}	877[c]	4.2
21	874	862	841	844	853	0.7	γ_{PhH}	859[c]	0.1
22	837	816	831	842	847	20.6	γ_{PhH}	847[c]	5.9
23	778	759	751	758	764	79.4	δ_{CCC}	767[i]	s
24	751	756	733	736	740	2.4	γ_{PhH}	754[i]	s
25	722	625	726	729	735	0.1	γ_{PhH}	732[i]	m
26	609	587	601	608	612	2.7	δ_{CCC}	598[e]	1.7
27	591	577	584	590	594	0.4	τ_{sk}, $\gamma_{C–C\equiv N}$	567[e]	1.7
28	562	510	565	570	575	1.4	δ_{CCC}, $\delta_{C–C\equiv N}$	560[e]	8.1
29	523	497	510	518	523	12.6	τ_{sk}, $\gamma_{C–C\equiv N}$	496[e]	0.1
30	472	473	474	479	486	3.9	δ_{CCC}, δ_{PhO}, $\delta_{C–C\equiv N}$	468[e]	0.4
31	418	421	411	418	424	0.0	τ_{sk}, $\gamma_{C–C\equiv N}$	463[e]	12.1
32	382	409	407	391.2	398	8.4	δ_{CCC}, $\delta_{C–C\equiv N}$	400[e]	w
33	329	384	384	391.0	377	116.1	γ_{PhOH}	378[j]	
34	261	281	257	266	272	0.3	τ_{sk}, $\gamma_{C–C\equiv N}$	[k]	m
35	182	209	174	183	192	2.5	δ_{CCC}, δ_{PhO}, $\delta_{C–C\equiv N}$	190[j]	
36	157	187	154	163	172	0.1	τ_{sk}, γ_{PhO}	[k]	

[a] B3LYP 6-31 + G(d,p).

[b] Measured after having decomposed the complex bands into components.

[c] Scaled, according to the correlation equations Nos. 6, 7, 8, 9 and 10 (Table 2), respectively.

[d] Vibrational modes: ν, stretching; δ, bendings, except out-of-plane ones; γ, out-of-plane bendings; τ, torsion; subscript sk, skeletal. For the atom numbering see Scheme 1.

[e] Solvent $CDCl_3$.

[f] A shoulder corresponding to free OH groups.

[g] OH groups, bonded intra-molecularly O–H$\cdots$N.

[h] A broad band, corresponding to OH groups, bonded intermolecularly O–H$\cdots$O.

[i] KBr disc. s, strong; m, moderate; w, weak.

[j] CsI disc.

[k] The band was not detected.

According to the calculations, vibration 1 (Table 3) is a pure $\nu_{O–H}$ mode. This vibration was studied repeatedly in connection with the conformers of various *o*-substituted phenols, including the title molecule [13–17]. For example, in very diluted CCl_4 solutions $\nu_{O–H}$ gives rise to two bands, at 3595 cm^{-1}, weak (*s-trans* **1b**, i.e. free) and 3559 cm^{-1}, strong (*s-cis* **1a**, intra-molecularly bonded) [15], and in argon matrices this band appears at 3576 cm^{-1} (**1a**) [17]. The concentrations of our $CHCl_3/CDCl_3$ solutions were relatively high (see Section 2), so we found three $\nu_{O–H}$ absorptions: a shoulder at 3586 cm^{-1} (**1b**, free), a band at 3559 cm^{-1} (**1a**, intra-molecularly bonded) and a broad band at 3311 cm^{-1}, corresponding to intermolecularly bonded O–H$\cdots$O. The relative intensities of these bands (Table 3) cannot give in-

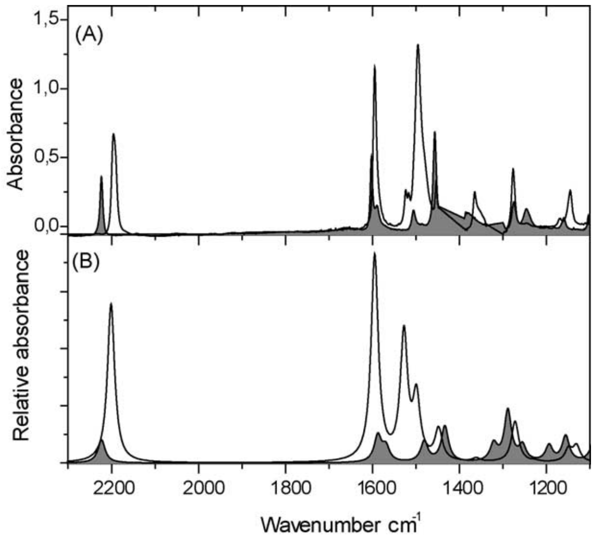

Fig. 1. (A) Experimental IR spectra ($0.15\,mol\,l^{-1}$ in DMSO) of 2-hydroxybenzonitrile (**1b**, shaded) and of its oxyanion (**6**, counter ion Na^{+}). (B) B3LYP 6-31 + G(d,p) (scaled by correlation equations nos. 10 and 15 (Table 2), respectively) spectra of the same species. Simulating the theoretical spectra by means of our program SimOpus [27] we postulated half-widths of $10\,cm^{-1}$ for all the bands.

formation about the **1a**/**1b** concentration ratio, as the stretching bands of hydrogen-bonded O–H, N–H, etc. groups are more intense (in cases of intermolecular hydrogen bonds they are very broad and much more intense) than the bands of the corresponding free (non hydrogen-bonded) groups [59]. We shall mention that if two *o*-hydroxybenzonitrile molecules form an intermolecular hydrogen bond, at least one of them has *s-trans* conformation. The **1b** $\nu_{O–H}$ frequency of $3586\,cm^{-1}$ (shoulder) is very close to that of the *p*-isomer ($3580\,cm^{-1}$ [60]) and practically coincides with $\nu_{O–H}$ of the *m*-isomer ($3587\,cm^{-1}$ [46]); their sharp bands were measured under the same conditions. The molecules of 3- and 4-hydroxybenzonitriles cannot form intra-molecular hydrogen bonds.

In DMSO/DMSO-d_6 solutions the **1b** molecules form very strong $O–H\cdots O= S(CH_3)_2$ bonds, manifested by a $\nu_{O–H}$ multiplet (over 10 bands) between 3200 and $2500\,cm^{-1}$, like $\nu_{O–H}$ of the *m*- [46] and the *p*- [60] isomers under the same conditions.

According to the calculations, the δ_{PhOH} coordinate is strongly delocalized, taking parts in vibrations 8, 11, 13, 15-17 (Table 3). On the contrary, γ_{PhOH} is well localized: vibration 33 is almost a pure γ_{PhOH} mode. This vibration was studied in detail by Carlson and coworkers [15,16], who measured the corresponding bands (saturated, $<0.01\,mol\,l^{-1}$ cyclohexane solutions) of **1a** at 392, $376\,cm^{-1}$ (Fermi-doublet) and of **1b** at $343\,cm^{-1}$, separately. For **1b** (Cs disc) we found this band at $378\,cm^{-1}$ (in the solid state the conformation is *s-trans* [31]).

The frequency of the cyano stretching band ν_{CN} of **1b** is a bit higher than ν_{CN} of the *p*-isomer, with: predicted $5\,cm^{-1}$ (B3LYP), measured $2\,cm^{-1}$; the corresponding integrated intensity A_{CN} (**1b**) however, is essentially lower than A_{CN} (*p*-isomer): predicted (B3LYP) and measured 1.7-fold (Table 3 and [46,60]). For the corresponding anions the *ortho*/*para* variations are qualitatively similar, viz. a ν_{CN} increase with: predicted $14\,cm^{-1}$ (B3LYP), measured $7\,cm^{-1}$; A_{CN} decrease: predicted 1.9-fold (B3LYP), measured 2.0-fold (Table 4 and [46,60]).

According to Katritzky and Topsom [61], the intensities of the aromatic skeletal bands *8a,b* and *19a,b* (Wilson's notation) can be used as a quantitative measure of the intra-molecular electronic interactions. For **1b** these are bands Nos. 7 (*8a*), 8 (*8b*) and 9 (*19*), both predicted and experimentally found (Table 3). Their total integrated intensity of $52.3\,kJ\,mol^{-1}$ is intermediate with respect to those of the *meta* ($46.4\,km\,mol^{-1}$ [46]) and *para* ($142.0\,km\,mol^{-1}$ [60]) isomeric hydroxybenzonitrile molecules.

The $\nu_{Ph–O}$ coordinate dominates in vibration 12, with predicted frequency $1274–1319\,cm^{-1}$ (ab initio, DFT, Table 3). We found the corresponding band at $1275\,cm^{-1}$ (DMSO-d_6) and $1304\,cm^{-1}$ ($CDCl_3$ and KBr). These frequencies are not away from the values of 1291, 1278 and $1285\,cm^{-1}$, measured for the *p*-isomer under the same conditions [60]. The corresponding vibration is also dominated by the $\nu_{Ph–O}$ coordinate, but the intensity of the latter band ($56.1\,mol\,l^{-1}$, solvent DMSO-d_6 [60]) is 4.3-fold higher than $A_{Ph–O}$ (**1b**) (cf. Table 3). All these values are reasonably higher (due to the HO/CN resonance, see Section 4.4.1) than the value of $1249\,cm^{-1}$, measured by Pinchas for the unsubstituted phenol in H_2O, and assigned as $\nu_{Ph–O}$ on the basis of the $15\,cm^{-1}$ $^{16}O/^{18}O$ isotopic shift [62]. Normal vibrations with essential contributions of the $\nu_{Ph–O}$ coordinate have been predicted near 1270 and $1256\,cm^{-1}$, and found at 1293 and $1243\,cm^{-1}$ (solvent DMSO-d_6) in the IR spectrum of 4-hydroxynitrobenzene [63].

4.3.2. *The 2-hydroxybenzonitrile oxyanion* 6

The theoretical and experimental IR data for the anion **6** are compared in Table 4. As above (Section 4.3.1), we can find there a good agreement between experimental and scaled theoretical frequencies. The m.d. between them for the ab initio methods used is $31.0\,cm^{-1}$, larger than the $14–28\,cm^{-1}$ interval of deviations, typical for nitrile anions [37] (and references therein). For the DFT calculations this deviation is ca. $16\,cm^{-1}$. This value is almost two-fold smaller than the ab initio one and also lies within the DFT deviation interval of $9–24\,cm^{-1}$, found for five nitrile anions [36–38,46].

The conversion of the 2-hydroxybenzonitrile molecule **1b** into the oxyanion **6** results in very essential changes in the IR spectrum (cf. Tables 3 and 4); some of them are well seen in Fig. 1. The changes are in a qualitative agreement between theory and experiment, e.g.:

1. Decrease in the cyano stretching frequency ν_{CN}: predicted $22\,cm^{-1}$ (B3LYP 6-31 + (d,p)), measured $29\,cm^{-1}$.

Table 4
Theoretical (HF 6-31G(d), MP2 6-31G(d), BLYP 6-31G(d) and B3LYP 6-31G(d), 6-31 + G(d,p) force field) and experimental (DMSO/DMSO-d_6) IR data for the 2-hydroxybenzonitrile oxyanion **6** (counter ion Na^+)

No.	HF	MP2	BLYP	B3LYP	B3LYP[a]	B3LYP[a]	Approximate description[d]	Experimental[b]	
	ν (cm^{-1})[c]	ν (cm^{-1})[c]	ν (cm^{-1})[c]	ν (cm^{-1})[c]	ν (cm^{-1})[c]	A (km mol^{-1})		ν (cm^{-1})	A (km mol^{-1})
1	3061	3072	3085	3075	3078	44.0	$\nu_{Ph\text{–}H}$	3075	4.2
2	3041	3060	3071	3063	3066	55.4	$\nu_{Ph\text{–}H}$	3058	2.4
3	3015	3033	3050	3043	3047	21.3	$\nu_{Ph\text{–}H}$	3042	3.6
4	3006	3016	3017	3014	3021	41.6	$\nu_{Ph\text{–}H}$	3016	8.5
5	2302	2101	2188	2218	2201	278.2	$\nu_{C\equiv N}$, $\nu_{C\text{–}CN}$	2194	65.8
6	1639	1649	1614	1627	1595	358.8	ν_{CC}, ν_{PhO}	1595	84.0
7	1585	1567	1550	1562	1528	220.6	ν_{CC}, $\nu_{Ph\text{–}O}$	1522	13.7
8	1518	1548	1502	1507	1499	107.7	ν_{CC}, δ_{PhH}	1496	207.1
9	1467	1481	1434	1461	1448	54.5	ν_{CC}, δ_{CCC}, δ_{PhH}	1453	14.1
10	1382	1387	1376	1373	1361	5.8	δ_{PhH}, δ_{CCC}	1364	46.2
11	1246	1343	1276	1275	1272	71.3	δ_{PhH}, ν_{CC}	1276	25.0
12	1209	1256	1224	1227	1227	2.0	δ_{CCC}, δ_{PhH}, ν_{CC}	1246	1.6
13	1143	1176	1157	1154	1149	21.9	δ_{PhH}, ν_{CC}	1169	4.3
14	1124	1159	1139	1133	1131	27.3	δ_{PhH}, ν_{CC}	1146	26.8
15	1056	1098	1081	1075	1076	0.9	γ_{PhH}, δ_{PhH}	1107	5.1
16	985	1042	1016	1012	1012	16.6	ν_{CC}, δ_{PhH}	1033[e]	w
17	978	867	915	923	937	0.3	γ_{PhH}	[f]	–
18	952	856	874	886	905	2.1	γ_{PhH}, τ_{sk}	863[e]	m
19	837	821	853	849	853	4.8	δ_{CCC}, ν_{CC}	[f]	–
20	835	783	817	820	823	17.0	γ_{PhH}, γ_{PhO}	841[e]	m
21	738	728	729	729	728	0.8	γ_{PhH}, γ_{PhO}, τ_{sk}	[f]	–
22	701	697	698	698	709	70.7	ν_{CC}, δ_{CCC}	748	m
23	684	621	692	692	704	2.6	γ_{PhH}, γ_{PhO}	728	s
24	594	611	598	597	600	1.9	δ_{CCC}, $\delta_{C\text{–}C\equiv N}$	598	m
25	577	585	579	578	581	1.2	$\gamma_{C\text{–}C\equiv N}$, τ_{sk}	570	m
26	543	528	546	560	566	2.1	δ_{CCC}, ν_{CC}	506	m
27	500	486	499	500	507	19.2	γ_{PhH}, τ_{sk}, γ_{Ph}	479	m
28	456	415	464	462	470	6.7	δ_{CCC}, δ_{PhO}, $\delta_{C\text{–}C\equiv N}$	454	m
29[g]	395	413	410	407	411	0.2	τ_{sk}, $\gamma_{C\text{–}C\equiv N}$	407	m

[a] B3LYP 6-31 + G(d,p).

[b] Measured after decomposing the complex band into components.

[c] Scaled, according to the correlation equations Nos. 11, 12, 13, 14 and 15 (Table 2), respectively.

[d] Vibrational modes: ν, stretching; δ, bendings, except out-of-plane ones; γ, out-of-plane bendings; τ, torsion; subscript sk, skeletal. For the atom numbering, see Scheme 1.

[e] KBr disc.

[f] The band was not detected.

[g] Followed by four lower-frequency vibrations.

2. Essential increase in the corresponding intensity A_{CN}: predicted 6.9-fold (same method), measured 2.7-fold.
3. Strong enhancement of the intensity of the aromatic skeletal bands of Wilson's *8* and *19* types; for **6** these are Nos. 6 (*8*), 7 (*19a*) and 8 (*19b*), both predicted and measured (Table 4). The sum of their integrated intensities of 304.8 km mol^{-1} is again intermediate between the values of 237.1 [46] and 421.0 [60] km mol^{-1}, measured for the *m*- and *p*-hydroxybenzonitrile anions, respectively. The intensity enhancement, caused by the **1b** → **6** conversion is: predicted 6.4-fold (B3LYP 6-31 + G(d,p)), measured 5.8-fold (Tables 3 and 4 and Fig. 1). The essential intensity enhancements of the *8* and *19* type bands, caused by conversions of molecules into carbanions, azanions and oxyanions [37,39,46,51,55,56] (and references therein) are examples for the strong effects of anionic substituents on these intensities [64]. Approximate quantitative measures of these effects on various IR frequencies and intensities [65–67] (and references therein) are the σ^+ constants of anionic substituents [68,69].
4. Unlike the preceding case (**1b**, $\nu_{Ph\text{–}O}$ at 1275 cm^{-1}), the $\nu_{Ph\text{–}O}$ coordinate of **6** is delocalized, participating to, but not dominating in vibrations 6 and 7, predicted within the 1614–1649 cm^{-1} and 1528–1585 cm^{-1} intervals (ab initio, DFT) and found at 1595 and 1522 cm^{-1} (in fact these are Wilson's *8a* and *19a* modes, but modified by the substantial participation of the $\nu_{Ph\text{–}O}$ coordinate, Table 4). Like in the case of the 4-hydroxybenzonitrile oxyanion [60] however, this shift of the $\nu_{Ph\text{–}O}$ coordinate to higher frequencies is obviously due to the strong shortening (hence strengthening) of the Ph–O bond, accompanying the conversion of the 2-hydroxybenzonitrile molecule into the oxyanion (cf. 4.4). For example, according to the calculations, the $\nu_{Ph\text{–}O}$ coordinate dominates in the vibration (nominally Wilson's *19a*) of the 4-nitrophenolate

anion, predicted near 1552 cm^{-1} and found at 1532 cm^{-1} (solvent DMSO-d_6) [63].

4.4. Structural analysis of the species studied

We shall follow the changes in both the steric and electronic structures, caused by the conversion of the 2-hydroxybenzonitrile molecule **1b** into the corresponding oxyanion **6**.

4.4.1. Steric structure

Certain calculated and measured geometry parameters of the species studied are compared in Table 5. As we mentioned above, in the monocrystal 2-hydroxybenzonitrile exists as infinite chains of molecules in *s-trans* conformation [31]. So, we included in Table 5 the geometry parameters, calculated for **1b** only. The following comments can be done on the corresponding data:

1. In fact all the methods used give good descriptions of the steric structure of the molecule **1b**. The m.d. values can usually [34–39,52,60] answer quantitatively for the question which one among the theoretical methods used gives the best description. For comparison: similar m.d.'s of 0.006-0.024 Å and 0.94–1.23° have recently been found for 4-hydroxybenzonitrile (same methods [46]). Of course nobody can expect a full coincidence between calculated (for isolated species) and X-ray (measured in the crystal state) geometry parameters.
2. The m.d. value ($\bar{\Delta}_i$) could give information on failures of most or all the methods used in the determination of a given structural element [38]. The $\bar{\Delta}_i$ values in Table 5 show that the methods used overestimate all the bond lengths, but the strong disagreement in the O–H case only ($\bar{\Delta}_i = 0.054$ Å) can be classified as a real failure. In fact, it is known that both ab initio and density functional calculations overestimate essentially the element–hydrogen bond lengths [70,71]. As the methods used give good descriptions of the structure of the molecule **1b**, we hope their structural predictions for the oxyanion **6** would also be adequate. So we should be able to follow the structural changes, accompanying the conversion of **1b** into **6**. The

Table 5
Theoretical (HF 6-31G(d), MP2 6-31G(d), BLYP 6-31G(d) and B3LYP 6-31G(d), 6-31 + G(d,p)), and experimental (X-ray) bond lengths (Å) and bond angles (degrees) in the *s-trans*-2-hydroxybenzonitrile molecule **1b** and in its oxyanion **6**

Species[a]	Molecule							Anion				
Methods	HF	MP2	BLYP	B3BYP	B3LYP[b]	X-ray[c]	$\bar{\Delta}_i$[d]	HF	MP2	BLYP	B3LYP	B3LYP[b]
C^1–C^2	1.441	1.433	1.435	1.431	1.432	1.431	*0.003*	1.433	1.428	1.427	1.422	1.424
$C^2\equiv N^3$	1.136	1.183	1.177	1.163	1.164	1.136	*0.029*	1.143	1.187	1.183	1.170	1.170
C^1C^4	1.394	1.406	1.424	1.411	1.411	1.394	*0.015*	1.444	1.456	1.485	1.468	1.465
C^1C^8	1.391	1.402	1.417	1.405	1.406	1.391	*0.013*	1.399	1.406	1.420	1.409	1.411
C^4C^5	1.387	1.396	1.408	1.398	1.399	1.387	*0.011*	1.452	1.448	1.467	1.456	1.454
C^5C^6	1.383	1.395	1.404	1.394	1.395	1.371	*0.023*	1.360	1.384	1.389	1.378	1.381
C^6C^7	1.387	1.396	1.408	1.397	1.399	1.378	*0.019*	1.412	1.408	1.424	1.414	1.416
C^7C^8	1.381	1.393	1.401	1.391	1.392	1.372	*0.020*	1.372	1.390	1.399	1.388	1.390
C^4–O^9	1.341	1.366	1.372	1.358	1.359	1.348	*0.011*	1.232	1.265	1.266	1.253	1.261
O^9–H^{14}	0.947	0.974	0.981	0.970	0.967	0.915[e]	*0.053*	–[g]	–[g]	–[g]	–[g]	–[g]
m.d.[f]	*0.0052*	*0.0180*	*0.0264*	*0.0156*	*0.0191*	*0.0000*						
$C^1C^2N^3$	178.05	178.28	179.21	179.18	178.37	179.15	*−0.53*	176.93	177.73	178.04	178.88	177.41
$C^2C^1C^4$	120.36	119.74	120.50	120.35	120.35	119.47	*0.79*	119.31	118.09	119.21	119.13	119.53
$C^2C^1C^8$	118.34	120.30	120.33	120.23	120.22	119.60	*0.28*	118.50	118.90	118.97	118.84	118.63
$C^4C^1C^8$	121.30	120.00	119.17	119.42	119.43	120.90	*−1.04*	122.20	123.00	121.82	122.03	121.84
$C^1C^4C^5$	119.46	119.52	119.69	119.59	119.65	118.38	*1.20*	113.37	112.81	113.22	113.21	113.68
$C^1C^8C^7$	119.23	120.20	120.80	120.72	120.69	119.79	*0.54*	122.10	121.10	121.72	121.75	121.71
$C^4C^5C^6$	120.01	120.11	120.22	120.19	120.16	120.08	*0.06*	122.75	123.39	123.31	123.20	122.99
$C^5C^6C^7$	120.94	120.52	120.58	120.65	120.64	121.60	*−0.93*	122.18	121.50	121.55	121.69	121.61
$C^6C^7C^8$	119.06	119.70	119.55	119.44	119.44	119.26	*0.18*	117.42	118.18	118.38	118.11	118.16
$C^1C^4O^9$	117.76	116.80	117.20	117.36	117.36	117.63	*−0.33*	124.11	123.75	123.76	123.81	123.68
$C^5C^4O^9$	122.78	123.70	123.11	123.06	122.98	123.99	*−0.86*	122.50	123.40	123.02	122.99	122.63
$C^4O^9H^{14}$	111.25	108.82	108.63	109.44	110.45	–[h]	–	–[g]	–[g]	–[g]	–[g]	–[g]
m.d.[f]	*0.687*	*0.633*	*0.789*	*0.700*	*0.765*	*0.000*	–	–	–	–	–	–

[a] For atom numbering see Scheme 2.

[b] B3LYP 6-31 + G(d,p).

[c] X-ray diffraction of a monocrystal [31].

[d] Mean algebraic deviation between theoretical and experimental values for a given structural element.

[e] Not included in the m.d. calculation.

[f] Mean absolute deviation (m.d.) between theoretical and experimental values for a given method.

[g] There is no H^{14} in the anion.

[h] No experimental data available.

strong disagreement in the O-H case ($\bar{\Delta}_\mathrm{i} = +0.053$ Å) may not be failure of the methods used. According to J. Hvoslof (Acta Crystallogr. Sect. B 24 (1968) 1431), the X-ray diffraction O-H bonds are systematically shortened by the decrement of 0.148 Å, compared to the neutron diffraction ones. So the real $\bar{\Delta}_\mathrm{i}$ for the O-H bond length becomes −0.095 Å and can be considered as a manifestaion of the intermolecular hydrogen bonds in the monocrystals, like in the case of 4-hydroxybenzonitrile [46].

3. Among the bond length changes, caused by the conversion of **1b** into **6**, the strongest are the shortening of the Ph–O bond with 0.10 Å and lengthenings of the adjacent CC bonds in the phenylene ring with 0.059 and 0.055 Å, respectively (mean values for the five methods used).
4. The conversion causes changes in all bond angles, but the anion **6** remains planar. The strongest bond angle changes take place at the oxyanionic center (−6.41° to +6.58°, mean values) and its *o*-positions (2.16°–3.03°, mean values).
5. Both the bond length and bond angle changes discussed are connected with the formation of a quasi-*ortho*-quinonoidal structure of the phenylene ring in the oxyanion.

4.4.2. Electronic structures

The MP2 6-31G(d) (Mulliken, in italics) and B3LYP 6-31 + G(d,p) (NBO, in bold) net electric charges q in the species studied, divided into fragments (cyano groups, phenylene rings and HO/O$^-$ groups) are shown in Scheme 2. Here are some comments on the corresponding data:

1. The dipole moment of 2-hydroxybenzonitrile (mainly **1a** in CCl_4 solutions) is 3.2 Debye [30]. The MP2 calculations performed give the value of 3.26 Debye for **1a**, and larger values, up to 3.7 Debye are obtained by the other methods used. So, we think that among the Mulliken charges, the MP2 ones are closest to the real charges in the title species.
2. The net charge changes $\Delta q = q_\mathrm{anion} - q_\mathrm{molecule}$ are usually quite informative to show the distribution of the new (carbanionic, oxyanionic, etc.) negative charge between individual fragments of the anions [37] (and many references therein). In the anion **6** studied, $\Delta q = q(\mathbf{6}) - q$ (**1a**) is distributed as follows (NBO Δq's in bold): *0.06*, **0.06** e$^-$ in the cyano group, *0.53*, **0.38** e$^-$ delocalize over the phenylene ring and *0.41*, **0.56** e$^-$ remain in the oxyanionic center. For comparison: in the oxyanionic centers of the 3- and 4-hydroxybenzonitrile anions remain *0.44*, **0.55** and *0.49*, **0.53** e$^-$ [46], respectively (same methods) of the oxyanionic charges.

5. Conclusion

We show in this work that the conversion of 2-hydroxybenzonitrile molecule into the corresponding oxyanion causes very essential IR spectral and structural changes. These changes, however, can be described and predicted adequately by both ab initio and density functional force field calculations.

Acknowledgements

The authors thank Prof. I.G. Binev, D.Sc, for the useful discussion. The financial support by the Bulgarian Council of Scientific Research for contract Chem.-1213 is also politely acknowledged.

References

[1] H. Finkelstein, J. Willems, I.G. Farbenind, A.G., German Patent 538,319 (1929).
[2] S. Ren, Environ. Toxicol. 17 (2002) 119.
[3] S.B. Mekapati, C. Hansch, J. Chem. Inform. Comput. Sci. 42 (2002) 956.
[4] A.O. Aptula, T.I. Netzeva, I.V. Valkova, M.T.D. Cronin, T.W. Schltz, R. Kuhne, G. Schuurmann, Quant. Struct.: Activity Relat. 21 (2002) 12.
[5] K. Carpenter, H.J. Cottrell, B.J. Heywood, W.G. Leeds, Mededel Landbonwhogesh. Opz., St. Gent 29 (1964) 644.
[6] H. Mizuno, N. Sakamoto, Y. Kinoshita, PCT Int. Appl. WO 02 24663 (Cl. C07D239/00), 28 March 2002.
[7] R.R. Wexler, C.G. Clack, J.M. Fevig, R.A. Galemmo, Q. Han, I.G. Jacobson, P.Y.S. Lam, H.Y. Li, D.Y.P. Pinto, PCT Int. Appl. WO 00 38683 (Cl. A61K31/495), 6 July 2000.
[8] K. Ueno, A. Ogawa, Y. Ohta, Y. Nomoto, K. Takaki, H. Kusaka, H. Yano, C. Suzuki, S. Nakanishi, PCT Int. Appl. WO 01 47931 (Cl. C07D487/14), 5 July 2001.
[9] T. Sakai, T. Senga, T. Furuta, A. Miwa, PCT Int. Appl. WO 01 47890 (Cl. C07D215/14), 5 July 2001.
[10] L.D. Arnold, J.W. Coe, T. Kaneko, M.P. Moyer, US 6130217 (Cl. 514-253 A61K31/495), 10 October 2000.
[11] D. Moye-Sherman, D. Cschneidner, PCT Int. Appl. WO 02 20466 (Cl. C07C255/00), 14 May 2002.
[12] S.-K. Choi, P.R. Fatheree, D.C. Green, D. Marquess, PCT Int. Appl. WO 02 57215 (Cl. C07C217/32), 25 July 2002.
[13] N.A. Puttnam, J. Chem. Soc. (1960) 5100.
[14] J.P. Segnin, F. Guillame-Vilport, R. Uzan, J.P. Poucet, J. Chem. Soc., Perkin Trans. 2 (1986) 773.
[15] G.L. Carlson, W.G. Fateley, J. Phys. Chem. 77 (1973) 1157.
[16] W.G. Fateley, G.L. Carlson, F.F. Bentley, J. Phys. Chem. 79 (1975) 199.
[17] J. Gebicki, A. Krantz, J. Am. Chem. Soc. 106 (1984) 8097.
[18] M. Broguier, F. Lahmani, A. Zehnacker-Rentien, V. Brenner, Ph. Millie, A. Peremans, J. Phys. Chem. A 105 (2001) 6841.
[19] S. Ram, B.K. Gupta, J.S. Yadaw, Indian J. Pure Appl. Phys. 19 (1981) 1110.
[20] B. Meyer, Ber. Deutsch. Chem. Ges. 26 (1893) 1254.
[21] M.W. Schmidt, K.K. Baldridge, J.A. Boatz, S.T. Elbert, M.S. Gordon, J.H. Jensen, S. Koseki, N. Matsunaga, K.A. Nguyen, S.J. Su, T.L. Windus, M. Dupuis, J.A. Montgomery, J. Comput. Chem. 14 (1993) 1347.
[22] C.C. Roothan, Rev. Mod. Phys. 23 (1951) 69.
[23] M.J. Frisch, M. Head-Gordon, J.A. Pople, Chem. Phys. Lett. 166 (1990) 275.
[24] M.J. Frisch, G.W. Trucks, H.B. Schlegel, G.E. Scuseria, M.A. Robb, J.R. Cheeseman, V.G. Zakrzewski, J.A. Montgomery Jr., R.E. Stratmann, J.C. Burant, S. Dapprich, J.M. Millam, A.D. Daniels, K.N.

Kudin, M.C. Strain, O. Farkas, J. Tomasi, V. Barone, M. Cossi, R. Cammi, B. Mennucci, C. Pomelli, C. Adamo, S. Clifford, J. Ochterski, G.A. Petersson, P.Y. Ayala, Q. Cui, K. Morokuma, D.K. Malick, A.D. Rabuck, K. Raghavachari, J.B. Foresman, J. Cioslowski, J.V. Ortiz, A.G. Baboul, B.B. Stefanov, G. Liu, A. Liashenko, P. Piskorz, I. Komaromi, R. Gomperts, R.L. Martin, D.J. Fox, T. Keith, M.A. Al-Laham, C.Y. Peng, A. Nanayakkara, C. Gonzalez, M. Challacombe, P.M.W. Gill, B. Johnson, W. Chen, M.W. Wong, J.L. Andres, C. Gonzalez, M. Head-Gordon, E.S. Replogle and J.A. Pople, Gaussian 98, Revision A.7, Gaussian, Inc., Pittsburgh, PA, 1998.

[25] A.D. Becke, Phys. Rev. A 38 (1988) 3098.

[26] A.D. Becke, J. Chem. Phys. 97 (1992) 9173.

[27] Y.I. Binev, Ph.D. Thesis, Bulgarian Academy of Sciences, Sofia, 2000.

[28] N.C. Santhosh, A.C. Nair, P.C. Mishra, Indian. J. Pure Appl. Phys. 36 (5) (1998) 264.

[29] F. Himo, L.A. Eriksson, M.R.A. Blomberg, P.E.M. Siegbahn, Int. J. Quant. Chem. 76 (2000) 714.

[30] C. Curran, E. Chaput, J. Am. Chem. Soc. 69 (1947) 1134.

[31] C. Beswick, M. Kubicki, P.W. Codding, Acta Crystallogr., Sect. C C52 (1996) 3171.

[32] I.G. Binev, B.A. Stamboliyska, E.A. Velcheva, Spectrochim. Acta Part A 52 (1996) 1135.

[33] I.G. Binev, B.A. Stamboliyska, Y.I. Binev, E.A. Velcheva, J.A. Tsenov, J. Mol. Struct. 513 (1999) 231.

[34] Y.I. Binev, C.T. Petkov, L. Pejov, Spectrochim. Acta Part A 56 (2000) 1949.

[35] B.A. Stamboliyska, Y.I. Binev, V.B. Radomirska, J.A. Tsenov, I.N. Juchnovski, J. Mol. Struct. 516 (2000) 237.

[36] Y.I. Binev, J.A. Tsenov, I.N. Juchnovski, I.G. Binev, J. Mol. Struct. (Theochem) 625 (2003) 207.

[37] Y.I. Binev, M.K. Georgieva, S.I. Novkova, Spectrochim. Acta Part A 59 (2003) 3041.

[38] S.I. Novkova, M.K. Georgieva, Y.I. Binev, Ch.Ts. Petkov, I.G. Binev, J. Mol. Struct. (Theochem) (2003) 167.

[39] E.A. Velcheva, B.A. Stamboliyska, Spectrochim. Acta Part A 60 (2004), in press.

[40] I.A. Koppel, J. Koppel, V. Pihl, I. Leito, M. Mishima, V.M. Vlassov, L.M. Yagupolski, R.W. Taft, J. Chem. Soc. Perkin Trans. 2 (2000) 1125.

[41] A. Fini, P. De Maria, A. Guarnjeri, L. Varoli, J. Pharm. Sci. 76 (1987) 48.

[42] R.M. Terkka, I.-H. Um, H.-Q. Xie, A.-P. Chatorouse, F. Terrier, S. Hoz, E. Buncel, J. Phys. Org. Chem. 11 (1998) 847.

[43] K. Kalfus, J. Socha, M. Vecera, Coll. Czech. Chem. Commun. 39 (1974) 275.

[44] M.K. Chantooni Jr., I.M. Kolthoff, J. Phys. Chem. 80 (1976) 1306.

[45] J.K. Ellington, E.M. Arnett, J. Am. Chem. Soc. 110 (1988) 7778.

[46] M.K. Georgieva, P.N. Angelova, I.G. Binev, J. Mol. Struct., 2004, in press.

[47] A. Bryson, R.W. Matthews, Aust. J. Chem. 16 (1963) 401.

[48] T.B. McMahan, P. Kebarle, J. Am. Chem. Soc. 99 (1977) 2222.

[49] R. Voets, J.-P. Francois, J.M.L. Martin, J. Mullens, J. Yperman, L.C. van Pouke, J. Comput. Chem. 11 (1990) 269.

[50] A.P. Scot, L. Radom, J. Phys. Chem. 100 (1996) 16502.

[51] B.A. Stamboliyska, E.A. Velcheva, I.G. Binev, Spectrochim. Acta Part A 59 (2003) 1541.

[52] M. Alcolea Palafox, Rec. Res. Dev. Phys. Chem. 2 (1998) 213.

[53] M. Alcolea Palafox, Spectrosc. Lett. 27 (1994) 1165.

[54] G. Leroy, M. Sana, C. Willante, D.R. Temsaman, J. Mol. Struct. 259 (1992) 369.

[55] I.G. Binev, J.A. Tsenov, E.A. Velcheva, I.N. Juchnovski, J. Mol. Struct. 344 (1995) 205.

[56] I.G. Binev, J.A. Tsenov, E.A. Velcheva, V.B. Radomirska, I.N. Juchnovski, J. Mol. Struct. 378 (1996) 133.

[57] I.D. Reva, S.V. Ilieva, R. Fausto, Phys. Chem. Chem. Phys. 3 (2001) 4235.

[58] O. Sala, N.S. Goncalves, L.K. Noda, J. Mol. Struct. 565–566 (1997) 411.

[59] G.N. Andreev, Molecular Spectroscopy (Bulg.), P. Khilendarski University Press, Plovdiv, 1999, p. 69.

[60] Y.I. Binev, J. Mol. Struct. (Theochem) 535 (2001) 93.

[61] A.R. Katritzky, R.D. Topsom, Chem. Rev. 77 (1977) 639.

[62] S. Pinchas, Spectrochim. Acta Part A 28 (1972) 801.

[63] I.G. Binev, R.R. Petrova, Y.I. Binev, Compt. Rend. Acad. Bulg. Sci. 50 (1997) 39.

[64] I.G. Binev, P.J. Vassileva, J. Mol. Struct. 114 (1984) 375.

[65] P.J. Vassileva, I.G. Binev, I.N. Juchnovski, Spectrochim. Acta Part A 39 (1983) 709.

[66] I.G. Binev, E.A. Velcheva, Spectrosc. Lett. 32 (1999) 793.

[67] E.A. Velcheva, I.N. Juchnovski, I.G. Binev, Spectrochim. Acta Part A 59 (2003) 1745.

[68] I.G. Binev, R.B. Kuzmanova, J. Kaneti, I.N. Juchnovski, J. Chem. Soc. Perkin Trans. II (1982) 1533.

[69] I.G. Binev, E.A. Velcheva, V.B. Radomirska, I.N. Juchnovski, Comput. Rend. Acad. Bulg. Sci. 47 (1994) 33.

[70] A.A. El-Azhary, H.U. Suter, J. Phys. Chem. 100 (1996) 15056.

[71] T.M. Kolev, B.A. Stamboliyska, Spectrochim. Acta Part A 58 (2002) 3127.